# LIMITATIONS OF ELECTRO-OPTIC MEASUREMENTS OF ELECTRON BUNCH LONGITUDINAL PROFILE

S.P. Jamison, ASTeC, STFC Daresbury Laboratory, UK
G. Berden, FELIX / FOM Institute Rijnhuizen, Nieuwegein, The Netherlands
W.A. Gillespie, P.J. Phillips, University of Dundee, Dundee, UK
A.M. MacLeod, University of Abertay Dundee, Dundee, UK

## *Abstract*

We provide quantitative comparisons of the fundamental limits of the principal techniques for electro-optic longitudinal profile measurements. The comparisons are based on simulations using the Coulomb field/optical field frequency mixing description of the electro-optic effect, with both time domain and spectral domain measurements considered. The important distinction between "temporal resolution" and "temporal limitation" which is encountered in the spectral measurements is highlighted by example. Effects of phase matching (or velocity mismatch of fields) in the detection crystal, the non-linear coefficient frequency response, and the choice of "balanced" or "crossed-polariser" detection are also considered.

## *Introduction*

In electro-optic (EO) detection of a bunch longitudinal profile, the bunch Coulomb field induces a temporal modulation in a probe laser intensity in an EO crystal. Three approaches to single shot EO detection have been demonstrated in accelerator diagnostics. The first and simplest, Spectral Decoding (SD), utilises a time-wavelength correlation within the input probe laser pulse, and a subsequent spectral measurement of the probe, to infer the temporal profile of the Coulomb field [1]. This use of a spectral measurement, and the inherent inseparability of temporal and spectral variations for ultrashort pulses ultimately prevents the application of this technique to very short bunch characterisation. The remaining techniques, Temporal Decoding (TD) and Spatial Encoding (SE), both measure the intensity modulation directly in the time domain through a time to space mapping. In TD this is done external to the accelerator beamline in an optical cross-correlator [2, 3]. In SE this is done within the electro-optic crystal itself [4]. While the practical implementations of TD and SE are quite distinct, the underlying encoding mechanisms are sufficiently similar to expect almost identical profiling capabilities for high energy beams. Here we evaluate the expected signals for spectral decoding and temporal decoding as a function of Coulomb field temporal profile. The applicability of the Temporal Decoding results to Spatial Encoding are discussed after a presentation of the simulation results.

The EO detection concept is traditionally described via an effective refractive index change induced by the Coulomb field. An alternative description based on the non-linear frequency mixing of Coulomb and optical fields allows for the analysis to be extended to chirped optical probe pulses and ultrashort Coulomb fields in a rigourous and straightforward manner. With this approach it can be shown that, in the small signal limit, the information of the Coulomb field temporal profile is encoded into principal axes polarisation components of the optical probe [5]:

$$\tilde{E}^{\mathrm{opt}}_{\mathrm{out}}(\omega) = \tilde{E}^{\mathrm{opt}}_{\mathrm{in}}(\omega) + i\omega a_{\omega}\tilde{E}^{\mathrm{opt}}_{\mathrm{in}}(\omega) * \left[\tilde{E}^{\mathrm{Coul}}(\omega)\tilde{R}(\omega)\right] \quad (1)$$

or equivalently

$$E^{\mathrm{opt}}_{\mathrm{out}}(t) = E^{\mathrm{opt}}_{\mathrm{in}}(t) + a_t \frac{\mathrm{d}E^{\mathrm{opt}}_{\mathrm{in}}(t)}{\mathrm{d}t}\left[E^{\mathrm{Coul}}(t) * R(t)\right] \quad (2)$$

In Eqns. 1-2, $\tilde{R}(\omega)$ and $R(t)$ are the response functions of the EO material in the frequency and time domain, respectively. The Coulomb fields and optical fields are denoted by e.g. $E^{\mathrm{opt}}_{\mathrm{out}}(t)$, $E^{\mathrm{Coul}}(t)$, with self evident subscripts. The coefficients $a_{\omega}, a_t$ are dependent on the particular polarisation arrangement of the optical and Coulomb fields, and the EO crystal orientation. The response function includes both phase matching and the frequency dependence of the nonlinear coefficient ($\chi^{(2)}(\omega)$ or $r_{41}(\omega)$). Although Eqns. 1-2 are only applicable to small signals, an extended description, which applies to strong fields or large signals, has recently been developed [6] and may be required when describing EO measurements of CTR or CSR.

## *Simulations*

Fig. 1 summarises simulations carried out for "balanced detection" and "crossed-polariser detection" setups, in a 100$\mu$m thick GaP EO crystal. For a given experimental arrangement Eqn 1 is used to describe the EO effect for each of the two orthogonal principal axis polarisation components. The effects of additional polarisation elements (waveplates and polarisers) are also evaluated for this pair of polarisation components. Finally, the (polarised) spectrum of the optical pulse can be evaluated. The complex spectrum is Fourier transformed into the time domain to find the associated temporal behaviour of the optical pulse, rather than using Eqn. 2. The simulations are taken to represent the "measured" spectra or temporal profile. Additional limitations arising from spectrometer resolving power (SD), the temporal resolution of the optical cross-correlator (TD) or the temporal-spatial imaging (SE) have not been considered as these are implementation specific and will usually represent secondary limitations. A Gaussian temporal profile in the Coulomb

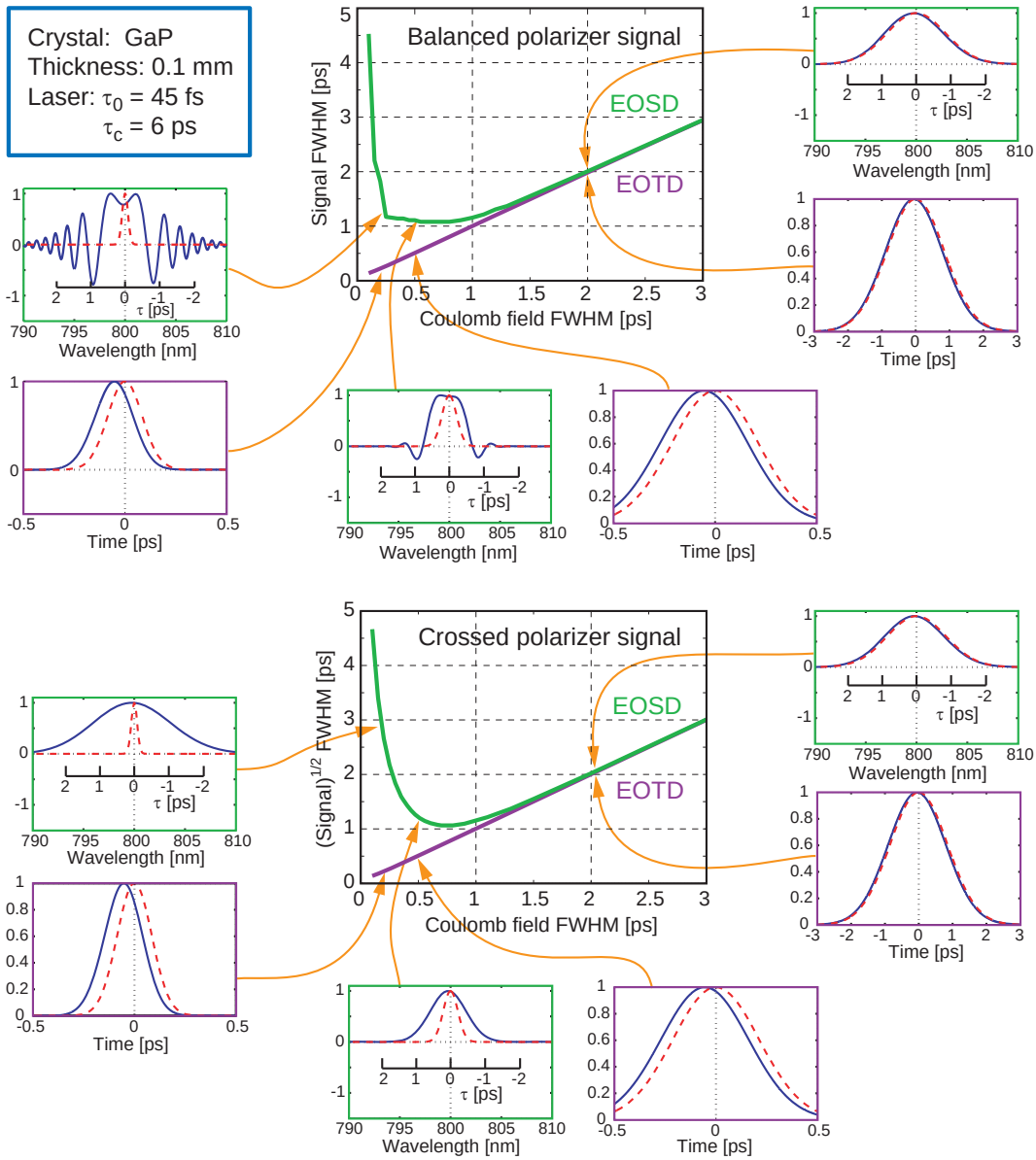


Figure 1: The "measured" Coulomb field FWHM durations as a function of the actual duration, for spectral decoding and temporal decoding, and for both crossed-polariser and balanced detection. The plots surrounding the balanced detection summary are examples of the signal $S(\omega)$ or $S(t)$ expected for EOSD and EOTD respectively. For crossed polariser detection, the examples show $[S(\omega)]^{1/2}$ and $[S(t)]^{1/2}$. The dashed red line shows the Coulomb field temporal profile.

field, with varying FWHM, was assumed in the calculations presented here. The phase-matching was evaluated for collinear Coulomb field and optical probe propagation. The probe laser was taken to be Gaussian (spectrally and temporally) with a transform limited intensity FWHM of 45 fs and central wavelength $\lambda = 800$ nm. A linear chirp was incorporated into the optical probe through a phase variation $E(\omega) \sim E_0(\omega)\exp(i\beta(\omega-\omega_0)^2)$. A value of $\beta = 0.05\,\mathrm{ps}/(\mathrm{rad.ps}^{-1})$, corresponding to a chirped pulse duration of 6.2 ps FWHM, was used in all calculations. The EO signal is taken as the difference in the (spectral or temporal) intensity, with and without the Coulomb field present, after all waveplates and polariser optics have been included. This difference signal is normalised by the input probe spectral or temporal profile. For balanced detection, for suitably long duration Coulomb fields, the normalised signal is proportional to the Coulomb field temporal evolution. i.e. $S(t) \equiv [I_{\mathrm{Coul}}(t) - I_{\mathrm{ref}}(t)]/I_{\mathrm{input}}(t) \propto E_{\mathrm{Coul}}(t)$. In the spectral domain a similar conclusion is obtained, with $S(\omega) \equiv [I_{\mathrm{Coul}}(\omega) - I_{\mathrm{ref}}(\omega)]/I_{\mathrm{input}}(\omega) \propto E_{\mathrm{Coul}}(\tau)$, where $E_{\mathrm{Coul}}(\tau)$ is the temporal variation of the Coulomb field mapped into the optical spectral domain according to $\tau \equiv 2\beta(\omega-\omega_0)$. For crossed-polariser geometry the signal instead scales quadratically with the Coulomb field, so that $S(t) \propto E^2_{\mathrm{Coul}}(t)$ and $S(\omega) \propto E^2_{\mathrm{Coul}}(\tau)$. To allow easy comparison between the "measured" and actual pro-

files, in Fig. 1 the FWHM of the signal, or square-root of the signal, is shown for balanced detection and crossed polariser detection calculations, respectively. Examples of the spectral and temporal signals are also presented to highlight the behaviour of the techniques for different Coulomb field temporal durations.

### *Spectral decoding*

Spectral decoding has specific limitations arising from the inseparability of temporal modulation and spectral content of the optical pulse. If an EO effect produces a fast temporal modulation in the optical probe, then it follows that a sufficiently broad spectrum is also produced. For very short pulses this induced spectral content distorts the input pulse chirp and invalidates the time-wavelength mapping that is to be used for the inference of the temporal variation. This aspect of spectral decoding produces a temporal limitation for characterising bunches; this limitation does not behave in the manner of an RMS time resolution, something which complicates the discussion of ultimate EO capabilities. As shown in Fig. 1 when the Coulomb field is suitably long the measurement produces an accurate representation of the field temporal profile. For very short bunches (typically less than 1 ps) the apparent profile is significantly broadened, even to beyond widths that would be expected to be faithfully measured, and it may also take on a apparent profile quite distinct from the bunch being measured. Hence, with SD it is useful define a temporal limitation as the width of the Coulomb field below which an accurate representation cannot be expected. This limitation is ultimately dependent on the probe pulse chirp, and can be shown to be $\tau_{\rm lim} = \sqrt{12\pi\beta}$. To convert this limitation into more familiar transform limited and chirped pulse durations, $\tau_0^{\rm FWHM}$ and $\tau_C^{\rm FWHM}$ respectively, requires specification of the spectral profile of the probe pulse. For the specific case of a pulse with a Gaussian spectrum, the SD limitation can be shown to be $\tau_{\rm lim} = 2.6\sqrt{\tau_0^{\rm FWHM}\tau_C^{\rm FWHM}}$. This implies that decreasing the transform limited pulse duration of the probe laser (or increasing its bandwidth) will allow higher time resolutions to be measured. However, it would require a $\tau_0^{\rm FWHM} < 10\,$fs pulse to obtain a 260fs limitation over a 1 ps window. For such a broadband pulse group velocity dispersion will however add significant additional complication, and potentially loss of time resolution, to any measurement.

### *Temporal measurements*

As seen in Fig. 1 the temporal measurements retain their validity for bunches significantly shorter than is possible for Spectral Decoding. For the example of TD with 100$\mu$m thick GaP it is found that a 100 fs FWHM Coulomb field will be "measured" with 130 fs FWHM (excluding any cross-correlator resolution limitations). For the temporal measurements the resolution limits are dominated by the material response, with the frequency dependence of the

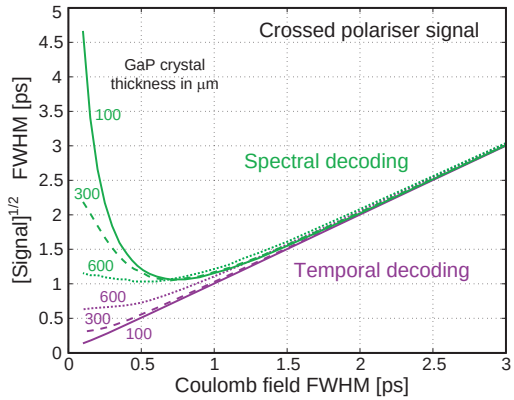


Figure 2: The effective measured bunch FWHM as a function of actual FWHM, for several thickness of GaP, and laser parameters as given in the text.

phase matching, the nonlinear coefficient, and the coupling of the Coulomb field into the detection crystal all playing a role. All of these effects arise from phonon resonances in the EO crystal, and the quantitative effects will differ between EO materials; amongst the materials that have been tested in accelerator diagnostics, GaP is currently obtaining the highest time resolution [3], principally because of the relatively high frequency of its first phonon resonance.

Fig. 2 shows the effect of material response on the measured signal for different thickness of GaP. In these simulations the phase matching was evaluated for collinear Coulomb and optical propagation, and the temporal measurements are therefore specific to temporal decoding. However, the non-collinear propagation inherent in spatial encoding, in the first instance, simply modifies the phase matching through an effective scaling of the optical propagation wavenumber. Through simulations with an effective non-collinear propagation it is found that broadly similar time resolution capabilities for SE and TD can be expected. Indeed, it is even found that for GaP and a $\lambda = 800\,$nm probe some improvement in phase matching can be expected for non-collinear propagation

## REFERENCES

[1] I. Wilke, A. M. MacLeod, W. A. Gillespie, G. Berden, G. M. H. Knippels, A. F. G. van der Meer. Phys. Rev. Lett. **88**, 124801 (2002)

[2] G. Berden, S. P. Jamison, A. M. MacLeod, W. A. Gillespie, B. Redlich, A. F. G. van der Meer. Phys. Rev. Lett. **93**, 114802 (2004)

[3] G. Berden, W. A. Gillespie, S. P. Jamison, E. A. Knabbe, A. M. MacLeod, A. F. G. van der Meer, P. J. Phillips, H. Schlarb, B. Schmidt, P. Schmüser, B. Steffen. Phys. Rev. Lett. **99**, 164801 (2007)

[4] A. L. Cavalieri, et al. Phys. Rev. Lett **94**, 114801 (2005)

[5] S. P. Jamison, A. M. MacLeod, G. Berden, D. A. Jaroszynski, W. A. Gillespie. Opt. Lett. **31**, 1753 (2006)

[6] S. P. Jamison. Appl. Phys. B **91**, 241 (2008)